Elke Goos, Christina Sickfeld, Fabian Mauß, Lars Seidel, Branko Ruscic, Alexander Burcat, Thomas Zeuch,
Prompt NO formation in flames: The influence of NCN thermochemistry,
Proceedings of the Combustion Institute, Volume 34 (2013) 657–666.

The original publication is available at www.elsevier.com

http://dx.doi.org/10.1016/j.proci.2012.06.128

The original publication is available at http://dx.doi.org/10.1016/j.proci.2012.06.128

Prompt NO formation in flames: The influence of NCN thermochemistry

Elke Goos[1*], Christina Sickfeld[2], Fabian Mauß[3], Lars Seidel[3], Branko Ruscic[4], Alexander Burcat[5], Thomas Zeuch[2*]

[1] Institute of Combustion Technology, DLR German Aerospace Center, Pfaffenwaldring 38-40, 70569 Stuttgart, Germany

[2] Institut für Physikalische Chemie, Georg-August-Universität, Tammannstr. 6, 37077 Göttingen, Germany

[3] Thermodynamics and Thermal Process Engineering, Brandenburg Technical University, 03046 Cottbus, Germany

[4] Chemical Sciences and Engineering Division, Argonne National Laboratory, Argonne, IL 60439, USA.

[5] Faculty of Aerospace Engineering, Technion IIT, Haifa 32000, Israel

Corresponding authors:
Email address: Elke.Goos@dlr.de (E. Goos) and tzeuch1@gwdg.de (T. Zeuch)

Keywords:
NCN heat of formation; NCN thermochemistry; Prompt NO formation; Methane flames, Acetylene flame

Abstract

The influence of the route via the NCN radical on NO formation in flames was examined from a thermochemistry and reaction kinetics perspective. A detailed analysis of available experimental and theoretical thermochemical data combined with an Active Thermochemical Tables analysis suggests a heat of formation of 457.8 ± 2.0 kJ/mol for NCN, consistent with carefully executed theoretical work of Harding et al. (2008) [5]. This value is significantly different from other previously reported experimental and theoretical values.

A combination of an extensively validated comprehensive hydrocarbon oxidation model extended by the GDFkin3.0_NCN-NO_x sub-mechanism reproduced NCN and NO mole fraction profiles in a recently characterized fuel-rich methane flame only when heat of formation values in the range of 445 - 453 kJ/mol are applied. Sensitivity analysis revealed that the sensitivities of contributing steps to NO and NCN formation are strongly dependent on the absolute value of the heat of formation of NCN being used. In all flames under study the applied NCN thermochemistry highly influences simulated NO and NCN mole fractions.

The results of this work illustrate the thermochemistry constraints in the context of NCN chemistry which have to be taken into account for improving model predictions of NO concentrations in flames.

1. Introduction

Prompt NO formation is a fascinating topic in combustion chemistry since the first report of the phenomenon by Fenimore [1] more than thirty years ago. The issue remained controversial until now. Fenimore attributed the residual NO observed close to burner surface in hydrocarbon flames to reactions involving molecular nitrogen and free radicals of hydrocarbons. He suggested the reactions

$$CH + N_2 \rightarrow HCN + N \qquad \text{(R1a)}$$

and

$$C_2 + N_2 \rightarrow CN + CN \qquad \text{(R2)}$$

as potential sources of NO formation.

Later an examination of prompt NO formation by Miller and Bowman [2] concluded that reaction (R1a) is responsible for the phenomenon.

However, studies of Cui et al. [3] and Moskaleva and Lin [4] changed the picture by showing that (a) the spin-orbit coupling in reaction R1a was not strong enough to account for experimental observations regarding prompt NO formation and that (b) the alternative product channel

$$CH + N_2 \rightarrow NCN + H \qquad \text{(R1b)}$$

may better account for the experimental results reported at that time. These findings sparked many consecutive studies providing evidence for the suggested new route. A central issue emerged - from experimental, theoretical and modeling perspectives - namely the value of the rate coefficient of R1b in the practically important temperature range around 1500 K. The extensive theoretical study on R1b by Harding et al. [5] agreed quantitatively with the shock tube study of Hanson and co-workers [6]. This finding clearly suggested that a central aspect of NCN reaction kinetics is settled. However, in their paper Harding et al. [5] pointed out that more accurate measurements of the heat of formation of NCN would significantly reduce the remaining uncertainty of their theoretical predictions below 2000 K. Considering the endothermicity of R1b it is obvious that the heat of formation for NCN is likewise a highly sensitive quantity for modeling predictions, when the NCN pathway for prompt NO formation

is implemented in reaction mechanisms. However, the relevance and extent of this uncertainty has not been systematically addressed [7,8,9]. So far reported values for the heat of formation of NCN differ by ~ 20 kJ/mol [10,11,12].

El Bakali et al. [7] suggested, based on NCN measurements in flames, using a rate coefficient significantly faster than Moskaleva und Lin´s value [4] but different from Harding et al. [5] and Vasudevan et al. [6]. In the more recent study of Lamoureux et al. [13] on CH, NCN and NO formation in fuel-rich methane and acetylene flames, the kinetic data of Hanson and co-workers for reaction (R1b) was used for kinetic modeling. The agreement of model predictions and experiment in this recent work also suggest a consistent picture regarding the modeling of prompt NO formation in methane flames.

However, all previous modeling studies on NO and NCN formation relied on kinetic models tested mainly for methane flames and much less for other fuels and other reactor types [7,8,9]. As a consequence the examination of a different fuel, e.g. acetylene in addition to methane, can imply using a different kinetic scheme [13] which is an unsatisfactory situation. Therefore it is highly desirable that up to date NO_x sub-mechanisms including NCN chemistry are implemented into general hydrocarbon oxidation models, which map the complete set of combustion features (ignition delay times, flame speeds, speciation in reactors and flames, engine modeling) and fuels (C1-C4 hydrocarbons, *n*-heptane, toluene, etc.).

This point leads to the main objectives of the present work. First, the quality of available thermochemical data of NCN will be critically analyzed accompanied by quantum chemical calculations using state of the art techniques. Second, a general hydrocarbon oxidation mechanism will be extended for simulating NO formation via the NCN pathway. Based on the analysis of NCN thermochemistry and using a comprehensive kinetic model the effect of different scenarios for the absolute value of the heat of formation of NCN in model predictions regarding NO formation in hydrocarbon flames will be tested and implications for modeling NO and NCN formation will be discussed.

2. Methods

(a) Thermochemistry

In order to use a consistent set of thermochemical data for kinetic modeling, enthalpies of formation obtained with the Active Thermochemical Tables (ATcT) [14,15] approach were employed whenever possible and used to update the Goos, Burcat and Ruscic thermochemical database [16]. The ATcT enthalpies of formation utilized the most current version [17] of the underlying Thermochemical Network (TN), which was recently engaged to produce new thermochemistry data for phenyl and halobenzenes [18], bromine oxides [19] and small hydrocarbon radicals [20]. In addition, the enthalpy of formation of NCN (CAS-number: 2669-76-3) was examined in detail and re-evaluated using ATcT, and NCN heat capacity, entropy, and enthalpy increment; and the corresponding polynomials [21,22] were recalculated within the rigid-rotor-harmonic-oscillator (RRHO) approximation using the PAC program of McBride and Gordon [23], based on spectroscopic data listed in Jacox [24].

(b) Kinetic model

The hydrocarbon oxidation model is the current version of a C1-C4 fuel base-mechanism first reported in [25]. The compilation strategy aims at continuously increasing the number and type of targets for mechanism validation. Important extensions were the inclusion of *n*-heptane oxidation at high and low temperatures [26], a methanol oxidation sub-mechanism developed by Dryer group (see [27] and literature cited therein) and the oxidation of toluene as reported in [28]. In the most recent work the mechanism was augmented by adding branched C4-species [29].

The current model is validated in the temperature range of 500-2300 K for the full set of targets of first reports [25,26] including flame speeds, ignition delay times, speciation in flames and reactors, soot precursor formation and HCCI engine ignition. The current range of fuels is methane, methanol, acetylene, ethylene, and ethane, propene and propane, *n*-butane and *iso*-butane, *n*-heptane, *iso*-octane and toluene.

For NO_x modeling different mechanisms available in the literature have been tested [8,9]. In the final hydrocarbon-NO_x mechanism the NO_x sub-model of the GDFkin3.0_NCN mechanism of the supplement of Lamoureux and coworkers [13] was used for extending our hydrocarbon mechanism. This NO_x-NCN sub-model is validated for recent measurements of CH, NCN and NO mole fraction profiles in methane flames and was previously used to extend other hydrocarbon oxidation models for NO_x predictions [30]. For assessing the influence of the heat of formation of NCN the effect of using different absolute values in model predictions was tested. We note that using

different thermodynamic databases for other nitrogen containing species [9,13] had only negligible effects on model predictions. Calculations were performed in a straightforward manner with the combined mechanism and the effect on predicting CH, NCN and NO mole fractions in various flames was analyzed.

The combined hydrocarbon-NO_x mechanism being used in the present study consists of 224 species. Nearly all reactions were written in a reversible way. Only some global irreversible reactions producing more than 2 products were written allowing only the forward reaction direction. If used thermochemistry data is applied for calculating the backward reaction rate coefficients and forward and backward reaction directions are counted separately as individual, irreversible reactions; then the mechanism would contain 2610 irreversible reactions. Kinetic, thermodynamic and transport data are available on request (contact: elke.goos@dlr.de or tzeuch1@gwdg.de).). The recommended thermodynamic data of NCN is provided as Supplementary data. All calculations were performed with the current version of the DARS software package [31].

3. Results and discussion

In the introduction it was hinted that thermochemistry of NCN requires a more detailed scrutiny. Available heats of formation of NCN are rather inconsistent (see Table 1). Therefore implemented NCN routes in kinetic models for predicting NO_x formation in flames may significantly depend on the value used in the thermochemical data set. The first part of this section will address this issue by re-examining the heat of formation of NCN within the context of Active Thermochemical Tables as well as previous experimental and theoretical work. Then the effects of NCN thermochemistry on prompt NO formation will be probed via flame simulations that use competing values for the enthalpy of formation of NCN. Finally, implications for modeling NO formation in flames will be discussed.

3.1 Thermochemistry of NCN

Taken *per se*, the temperature-dependent enthalpy increment, heat capacity, and entropy of NCN can be calculated reasonably well, because the influence of uncertainties in molecular properties of NCN is small in comparison to inconsistencies in the values for the heat of formation of NCN at standard conditions $\Delta_f H°(NCN)$. Gurvich et al. [32] and JANAF Tables [33] provide $\Delta_f H°_{298K}(NCN) = 501 \pm 25$ kJ/mol and 473 ± 21 kJ/mol, respectively, although they are based on the same approximate determination [34]. NIST WebBook [35] reports only the JANAF value and ignores Gurvich et al. and two newer results: the lower semi-experimental value $\Delta_f H°_{298K}(NCN) = 451.8 \pm 16.7$ kJ/mol of Clifford et al. [10] (from experimental electron affinity of NCN and theoretical gas-phase acidity of HNCN), and the more accurate but higher value of Bise et al. [11], who reported $\Delta_f H°_{0K}(NCN) = 466.0 \pm 2.9$ kJ/mol, equivalent to $\Delta_f H°_{298K}(NCN) = 466.5 \pm 2.9$ kJ/mol (from the N-CN bond dissociation energy and the N_2 elimination energy from NCN). Ignoring the older values from Gurvich and JANAF, the two newer choices for an experimentally based $\Delta_f H°_{298}(NCN)$ are nearly exclusive in the sense that their uncertainties do not provide a convincing overlap between the alternatives.

Very recently Canneaux et al. [12] examined NCN by several theoretical methods (CBS-QB3, CBS-APNO, G3//B3LYP, G3, and G4), and obtained $\Delta_f H°_{298}(NCN) = 448.7 \pm 3.4$ kJ/mol as a weighted average, which favors the lower value of Clifford et al. [10] and directly negates the value of Bise et al. [11]. Pertinently, Clifford et al. [10] have accompanied their experimental effort with CBS-APNO calculations, which produced $\Delta_f H°_{298K}(NCN) = 453$ kJ/mol, in line with their semi-experimental value. Similarly, our own calculations at the G3, G3//B3LYP, CBS-Q, CBS-QB3, and CBS-APNO levels of theory suggest enthalpies of formation in the 443–452 kJ/mol range, in apparent support of the lower value of Clifford et al. [10]. However, earlier on, Martin et al. [36] have conducted

CASSCF and CCSD(T) computations and selected a ZPE-uncorrected atomization energy of 1208 ± 8 kJ/mol, which implies $\Delta_f H°_{298K}$(NCN) = 465 ± 8 kJ/mol, supporting (and predating) the higher value of Bise et al.[11].

In such situations, ATcT is usually capable of successfully arbitrating between inconsistent values by exploiting redundant thermochemical cycles in the Thermochemical Network (TN), providing that the body of thermochemically-relevant data is sufficiently rich. The TN includes the experimental determinations discussed above: electron affinity measurements of Clifford et al. [10] and Taylor et al. [37] as well as Bise et al.´s [11] determinations of the N-CN bond dissociation energy and N_2 elimination energy to triplet and singlet carbon. These are complemented by the available theoretical determinations: total atomization energy of Martin et al. [36] together with their isomerization energies to CNN and cyclic NCN at the ROHF-CCSD(T)/pVTZ level of theory, the CBS-APNO results of Clifford et al. [10], as well as our own G3, G3//B3LYP, CBS-Q, CBS-QB3, and CBS-APNO computations of total atomization energy of NCN, energy of N_2 elimination to form triplet C, and N-CN bond dissociation energy, and G3//B3LYP electron affinity, ionization energy, and energies of isomerization to CNN and cyclic NCN. Apparent abundance notwithstanding, the resulting number of thermochemical cycles involving NCN is meager when compared to most other chemical species in the TN, connecting relatively weakly to the rest of the TN. This makes the resulting ATcT value highly tentative, at best. Indeed, based on this TN, the ATcT approach suggests $\Delta_f H°_{298}$(NCN) = 445.73 ± 1.70 kJ/mol, even lower than the value of Clifford et al. [10] and in apparent full agreement with Canneaux et al.´s value [12].

ATcT analysis of the provenance indicates that the value is dominated by single-reference computational results in the TN. The analysis also exposes some weaknesses of the experimental data: the determination [34] responsible for early values [32,33] is significantly less accurate than believed, the electron affinity measurements [10,37] cannot influence the value of NCN without involving a theoretical gas-phase acidity, and the three thresholds of Bise et al. [11] appear to be less then fully mutually consistent irrespective of the assumed value for NCN. Thus, single-reference computations, which do appear mutually consistent when taken at face value, statistically prevail. However, an inspection of these computations reveals that single-reference descriptions of the $^3\Sigma^-_g$ ground state of the NCN biradical suffer from spin contamination, although the effect on the computed energies is not immediately clear. The spin contamination problem has escaped the attention of Canneaux et al. [12] and Clifford et al. [10]. Unfortunately, the accuracy by which multireference methods reproduce energies generally lags behind that of single-reference methods, even when one juxtaposes state-of-the-art multireference methods with middle-of-the-pack single-reference methods. Indeed, though Martin et al.[36] explored a multireference

approach, they chose to produce their final result with single-reference based CCSD(T)/pVTZ using restricted-open wavefunctions in order to limit spin contamination.

Clearly, in order to produce a reliable enthalpy of formation of NCN and resolve the controversy between low and high values, ATcT needs additional thermochemically-relevant information. Luckily, Harding et al. [5] have recently examined the potential energy surface of the CH + N_2 reaction using multireference methods (CASPT2 and internally contracted CAS+1+2 with and without Davidson correction), as well as restricted-open CCSD(T). Though the latter is similar to the approach of Martin et al. [36], Harding et al. [5] have used larger basis sets and extrapolated the results to the complete basis set limit. They found very good agreement between CAS+1+2+QC and CCSD(T) energies for all stationary points having a small T_1 diagnostic (<0.02). The agreement and smallness of the T_1 diagnostic infuses additional confidence in their final RO-CCSD(T)/CBS//CASPT2/aug-cc-pVTZ ZPE-corrected energies for $^2CH+N_2 \rightarrow H+NCN$ (81.8 kJ/mol), $^4CH + N_2 \rightarrow H + NCN$ (8.7 kJ/mol), and $H + NCN \rightarrow HCN + N$ (-17.37 kJ/mol). When analyzed by ATcT as a localized TN [38,39] focused on NCN and aided with ATcT auxiliary thermochemistry for doublet and quartet CH (see also Ref. 40), N, H, and HCN; one finds that all three reaction energies are remarkably mutually consistent, showing that Harding et al. [5] also seem to correctly reproduce (within $\leq$ 1.7 kJ/mol) both the doublet-quartet splitting in CH and the reaction enthalpy of $CH + N_2 \rightarrow HCN + N$ (both independent of NCN). The ATcT result from this localized TN is $\Delta_f H°_{298}$(NCN) = 457.8 ± 2.0 kJ/mol, and represents the best currently available value. This enthalpy of formation is within the error bars of earlier theoretical result of Martin et al. [36] and refines it substantially, though it appears to no longer fully support the experimental result of Bise et al. [11].

The conclusion seems to be that single-reference based theoretical results produce enthalpies of formation of NCN that are decisively too low and tend to bias the ATcT analysis if taken at face value. The ATcT analysis reveals that available experimental determinations, which produce higher enthalpies of formation of NCN, are not as internally consistent as one would have initially hoped. Thus, the most credible value appears to emanate from the ATcT approach that relies on results from restricted-open coupled cluster methods, in lieu of as-yet-not-developed highly accurate multireference theoretical methods.

3.2 Modeling of CH, NCN, and NO mol fraction profiles in flames

In recent years many experimental and theoretical studies on the NCN and NO formation in flames have been reported [7,8,9,13,30, and literature cited therein]. The recent work of Lamoureux et al. [13] on NO and NCN

formation in laminar premixed burner stabilized fuel rich methane and acetylene flames at 40 Torr is the central reference for the present study. Flame data including temperature profiles reported in this study are used in present work. In the same study an updated NO_x mechanism is provided which, as explained above, is combined with our general hydrocarbon oxidation mechanism. We note that also Turanyi et al. [30] used the GDF_Kin mechanism in their uncertainty analysis of NO formation in flames.

Since the CH radical is a crucial precursor of NCN via reaction (R1b) an accurate simulation of this species is an important precondition for assessing NO formation via NCN in modeling studies. The upper panel of Fig. 1 shows the good agreement between the predicted and experimental CH mole fraction profiles, which is independent of the applied $\Delta_fH°_{298K}$(NCN) value. The slight overprediction by 15% is clearly within the experimental uncertainty. This is an important finding since CH mole fractions were, until now, not a target in the development of our multi-fuel model. It supports our compilation strategy aiming at comprehensive mechanisms whose application is not strictly limited to the targets of validation [25,26,41].

In the following, this mechanism will be used to elucidate the effect of NCN thermochemistry within the different NCN heat of formation scenarios (Case I: $\Delta_fH°_{298K}$(NCN) = 445.7 kJ/mol case II: 466.9 kJ/mol, case III: 457.8 ± 2.0 kJ/mol, case IV: NCN thermodynamical data of GDF_KIN 3.0 mechanism, $\Delta_fH°_{298K}$(NCN) = 450 kJ/mol, slightly different heat capacities). The upper and lower panels of Fig. 1 show predicted NCN and NO concentrations for the different cases. The first observation is that predicted NCN and NO profiles differ significantly between the scenarios peaking for the GDF_KIN thermodynamical data (Case IV) and showing the lowest concentrations for Case II with the highest NCN heat of formation. Already at this stage it becomes clear that a serious problem for NO_x modeling arises. When NO and NCN predictions differ to such an extent, the relative sensitivities of reactions on the pathways leading to NO formation will be affected. This is illustrated in Fig. 2, where the most sensitive reactions for NO formation within the NO_x chemistry are shown for Cases I -IV. The surprising result is that not only the absolute sensitivities differ significantly (NCN-sensitivities) but also the ranking of sensitive reactions involving nitrogen chemistry has changed in case of sensitivities for NO. Reaction (R1b) is only for Case I the most sensitive reaction for NCN and NO formation and also the sensitivities for NCN + O and NCN + H are affected. The most sensitive reactions of the baseline hydrocarbon mechanism are also shown in Fig. 2, but their sensitivities remain largely unchanged. We note that for the sensitive CH_3 + O reaction the results of our extensive experimental study were used in the kinetic model [42].

At higher equivalence ratios the sensitivity of the thermochemistry of NCN on NO prediction is stronger due to increased CH concentrations which imply more NO formation via reaction $CH + N_2 = NCN + H$ (R1b).

In principle the effect of temperature is also profound, as the backward reaction rate of reaction (R1b) is highly sensitive on the NCN thermochemistry.

The differences shown in Figs. 1 and 2 are almost as significant as the differences being observed by Turanyi and co-workers [30]: They compared reaction sensitivities for NO formation using different NO_x mechanisms featuring either R1a or R1b as the route leading to prompt NO.

Interestingly, the very reasonable decision of Turanyi and co-workers [30] to use a consistent thermochemical dataset has led to a confusing situation. Their use of the GDF_KIN mechanism as a basis for their uncertainty analysis is motivated by the good performance of this model regarding the simulation of NO formation via NCN. But this is only true within the case I or case IV/ GDF_KIN thermodynamical data scenario as we have illustrated in Fig. 1, but not for the Case III scenario which applies for the work of Turanyi and co-workers [30].

The implication is drastic: When the value of the NCN heat of formation recommended in the present study ($\Delta_f H°_{298K}$(NCN) = 457.8 kJ/mol, Case III) prevail, many conclusions of modeling studies on prompt NO formation via NCN become questionable and have to be reexamined.

A short literature survey for existing hydrocarbon oxidation mechanisms featuring NO_x sub-models reveals that both high and low enthalpies of formation of NCN (Cases I and II) are commonly used (see Table 1). We further note that NCN and NO concentration are ca. 20% lower when, instead of the Case IV/GDF_KIN scenario, our representation of heat capacities is used together with $\Delta_f H°_{298K}$(NCN)=450 kJ/mol.

In Fig. 3 the modeling results for the acetylene flames being examined by Lamoureux et al. [13] are shown. We see in the left panels that for the stoichiometric case a satisfactory agreement is found. However, the NO mole fraction is slightly underpredicted for Case I and IV and more severely for Cases II and III. The peak concentrations of CH and NCN are captured quite well while the positions are slightly shifted in our model prediction. For the fuel rich flame (right panels of Fig. 3) both the CH and NCN mole fractions are overpredicted for all cases. Taking into account that CH mole fractions in acetylene flames were not a target of our model, the agreement is still satisfactory.

In the modeling part of Lamoureux et al.´s work [13] the Skevis and Lindstedt acetylene mechanism [43] was used being augmented by the NO_x sub-mechanism of the GDF_Kin 3.0 model. This model showed the same tendency to overpredict CH in the fuel rich flame but captures better the CH and NCN peak positions (not shown here, see Fig. 11 in [13]). The most intriguing point, however, is the following: Lamoureux et al. found with this model a significant underprediction of NCN concentration for both flames. This finding was rationalized by proposing alternative routes to NCN formation like $C_2O + N_2 \rightarrow NCN + CO$. Adding the same NO_x sub-mechanism to our general hydrocarbon oxidation model results in acceptable agreement for the predicted CH, NCN and NO mole fraction profiles for the stoichiometric flame (when the heat of formation issue is ignored for a moment). The overprediction of NO and NCN in the Case I and IV scenarios for the fuel rich flame rather points to difficulties in modeling CH mole fraction profiles and does not indicate missing NCN chemistry. The different model predictions are most probably related to significant differences of the models in predicting the mole fractions of H and O atoms, which consume NCN.

These findings call for improving our capability of modeling CH as well as H and O atom mole fractions in acetylene flames, and focus our intention on the predictive power of single fuel and single reactor type models when the range of test cases is extended. The very broad target range of the general hydrocarbon oxidation mechanism limits systematic difficulties in predicting H and O atom concentrations.

However, for settling the issue of additional routes to NCN, the further examination of speciation in acetylene by comprehensive models seems necessary.

4. Conclusions

In the present study the thermochemistry of NCN and its role for model predictions of NO formation in flames has been critically analyzed. The detailed inspection of the recent high level calculations of Harding et al. [5] of the hypersurface for reaction (R1b) combined with the Active Thermochemical Tables analysis indicates that a heat of formation $\Delta_f H°_{298K}(NCN) = 457.8 \pm 2.0$ kJ/mol for NCN leads to a consistent picture from a state of the art theoretical perspective. This value differs significantly, however, from other previously reported experimental [11] and theoretical values [12, 36].

The kinetic modeling part of this work illustrated that model predictions based on an established comprehensive multi-fuel hydrocarbon oxidation model [25,26,29] being extended by the recently updated NO_x sub-mechanism of the GDF-Kin model [13] can in principle reproduce CH, NCN and NO profiles in a recently characterized fuel-rich methane flame [13]. However, the agreement of model predictions for NCN and NO mole fraction profiles in the present and several other previous literature studies for various flames is only given when the applied heat of formation of NCN in the thermochemical database is close to or below the value being reported by Clifford et al. [10] being around 450 kJ/mol. In case the more recently reported value of Bise et al. [11] (466.9 kJ/mol) or the recommended value of the present study (457.8 kJ/mol) is used, the model predictions differ significantly from the experimental references. In addition the ranking and the absolute value of reaction sensitivities are significantly changed when the NCN heat of formation is altered.

We therefore have to conclude that current understanding of prompt NO formation might be based on model predictions which used in general rather improper representations of NCN thermochemistry.

In a future effort we therefore will look carefully on the reaction kinetics of prompt NO formation to develop a comprehensive kinetic model in agreement with thermochemistry constraints.

Acknowledgements:

Funding by the Energy Program of the German Aerospace Center (DLR) is gratefully acknowledged by E.G. Funding by the Fonds der Chemischen Industrie is gratefully acknowledged by T.Z. The work at Argonne National Laboratory was performed under the auspices of the U.S. Department of Energy, Office of Basic Energy Sciences, Division of Chemical Sciences, Geosciences, and Biosciences, under Contract No. DE-AC02-06CH11357. E.G., F.M., L.S. and T.Z. acknowledge support from COST Action CM0901: “Detailed chemical kinetic models for cleaner combustion”.

Appendix A: Supplementary data (Thermochemistry data of NCN)

Supplementary data associated with this article can be found in the online version at

http://dx.doi.org/10.1016/j.proci.2012.06.128

and in front of the references, near the end of this file

Fig. 1:

Simulated and measured mole fraction profiles of CH, NO (upper panel) and NCN (lower panel) in a fuel rich CH_4-O_2-N_2 flame: Φ=1.25, x(CH_4)=0.124, x(O_2)=0.198, x(N_2)=0.678; for experimental details see [13]. Cases I-IV: Δ_fH_{298}=445.7 kJ/mol (I), Δ_fH_{298}=466.5 kJ/mol (II), Δ_fH_{298}=457.8 kJ/mol (III), Δ_fH_{298}=450.0 kJ/mol (IV).

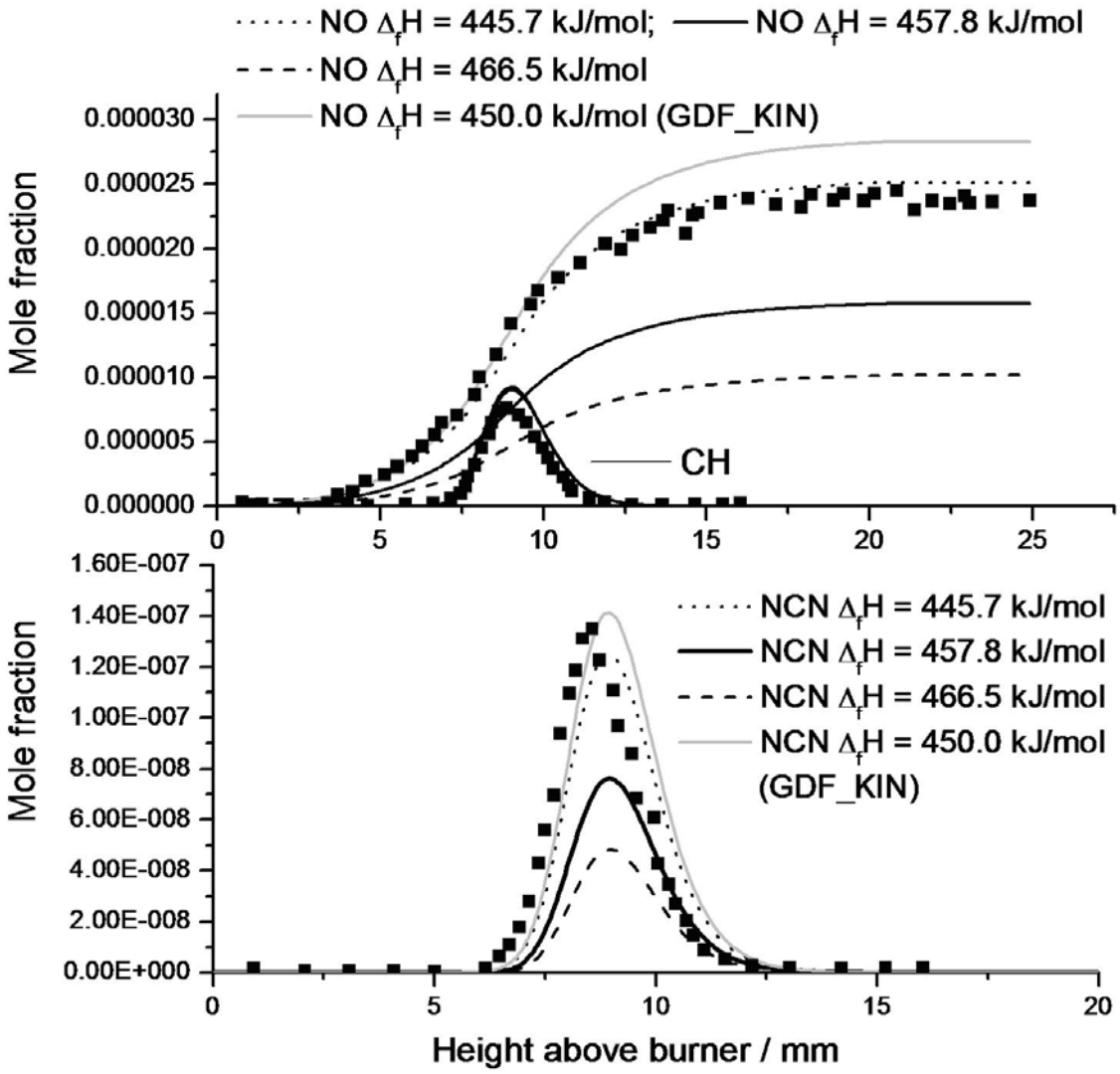

The original publication is available at http://dx.doi.org/10.1016/j.proci.2012.06.128

Fig. 2:

Relative reaction sensitivity coefficients for the mole fractions of NO (upper panel) and NCN (lower panel) of a fuel rich laminar methane (ϕ = 1.25) [13] for different heat of formation of NCN.

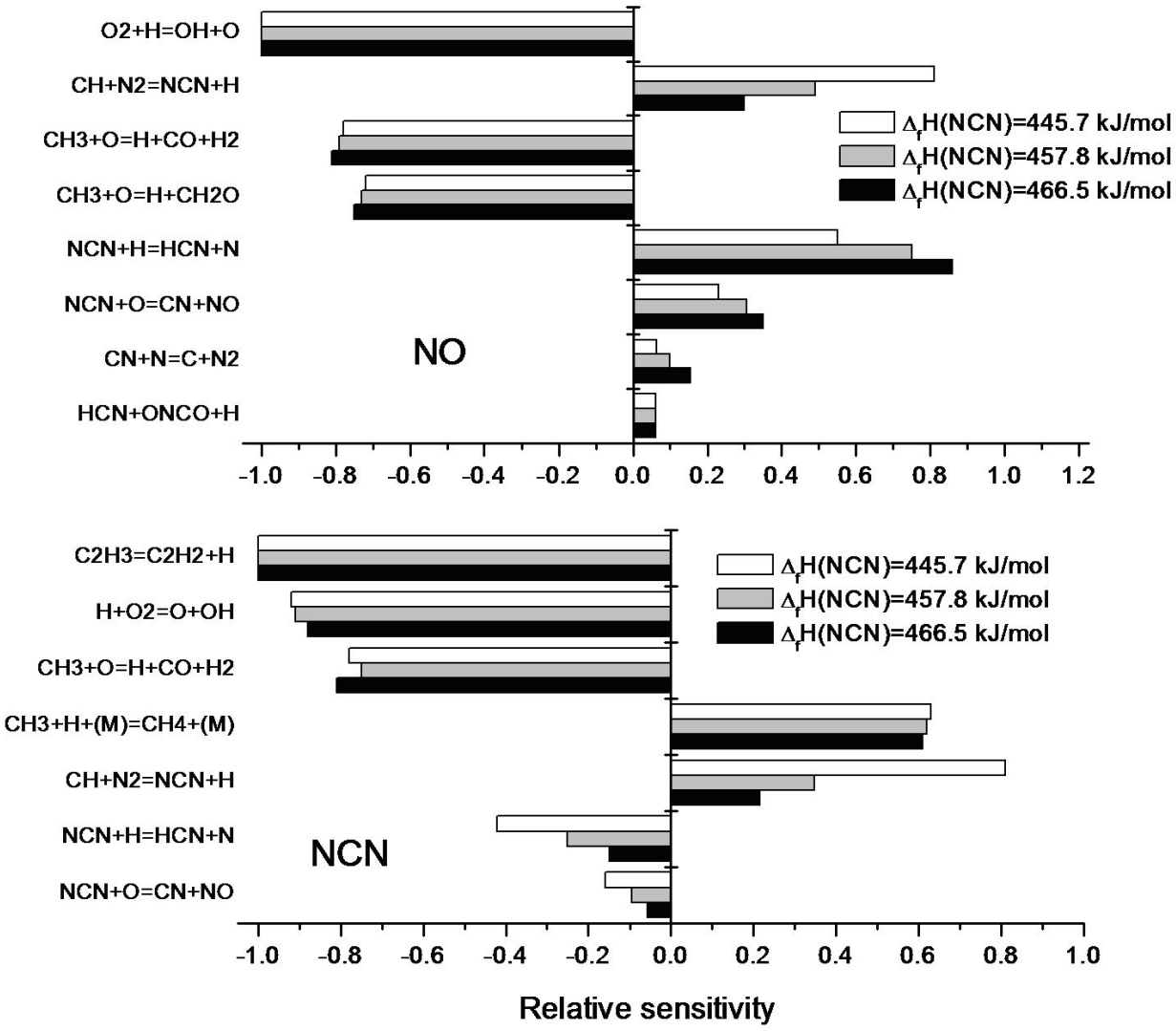

The original publication is available at http://dx.doi.org/10.1016/j.proci.2012.06.128

Fig. 3:

Simulated and measured mole fraction profiles of CH, NO (upper panels) and NCN (lower panels) in acetylene-air flames ([13]). Stoichiometric flame: Φ=1.0, x(C_2H_2)=0.067, x(O_2)=0.167, x(N_2)=0.766. Fuel rich flame: Φ=1.25, x(C_2H_2)=0.0826, x(O_2)=0.165, x(N_2)=0.753; for experimental details see [13]. Cases I-IV: Δ_fH_{298}=445.7 kJ/mol (I), Δ_fH_{298}=466.5 kJ/mol (II), Δ_fH_{298}=457.8 kJ/mol (III), Δ_fH_{298}=450.0 kJ/mol (IV).

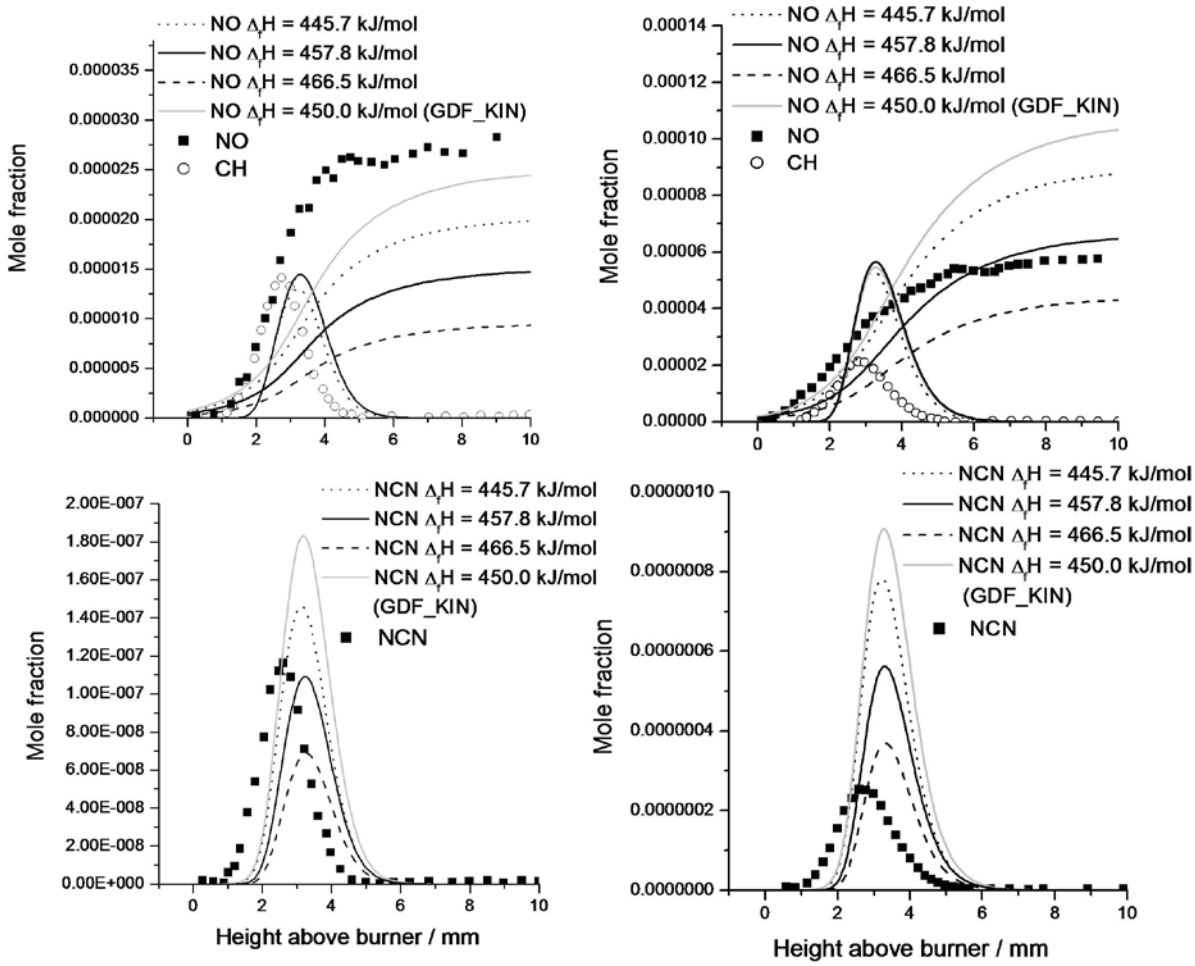

Table 1:

Experimental and calculated Standard Heat of Formation of NCN and its usage in some modeling studies

$\Delta_f H°_{298K}$(NCN) kJ/mol	Experimental or calculated values	Used in prior modeling studies
501 ± 25	Gurvich [32]	NASA program CEA and Thermo Build [44a] with NCN data from [44b].
473 ± 21	JANAF [33], listed by NIST Webbook [35]	Zamansky and Lissianski [45]
465 ± 8	Martin et al. [36] multireference methods (recalculated from atomization energy)	
466.5 ± 2.9	Bise et al. [11] (recalculated from $\Delta H_f°_{0K}$ = 466.0 ± 2.9 kJ/mol)	Garner et al. [46], Konnov [9], Vasudevan et al. [6], Zhu et al. [47].
464	Moskaleva, Lin [4], Mebel et al.[48]	Gersen et al. [49] modified GRI mechanism
Unknown value		Sepman et al. [50]
459	Harding et al. [5] multireference methods (calculated from reaction endothermicity of $CH+N_2 \rightarrow NCN+H$)	
457.8 ± 2.0	**This work, recommended value**	
451.8 ± 16.7	Clifford et al.[10]	Benard et al.[51], El Bakali et al.[7], Lamoureux et al. (107.7 kcal/mol) [13], Xu and Lin [52], Zhu et al. [53].
450 - 450.2	Melius [54]	Dagaut, Glarborg and Alzueta [55a], Sarathy et al. [55b], all LLNL mechanisms published before December 2011: e.g. [56]
448.7 ± 3.4	Canneaux et al. [12], weighted average of single reference methods	
444.5	Dammeier and Friedrichs [57] (calculated from $\Delta H_f°_{0K}$ = 444 kJ/mol)	
443 – 452	This work, single reference methods	

The original publication is available at http://dx.doi.org/10.1016/j.proci.2012.06.128

The References are at the end of the file

Supplementary data:

Thermochemical data of NCN with heat of formation at 298K = 457.8 kJ/mol in 9-term-NASA-format:

```
 NCN               HF298=457.8+/-2.0 kJ  REF=ATcT D 2012
3 T 1/12 N   2.00C   1.00    0.00    0.00    0.00 0   40.0241800     457800.000
     50.000   200.000 7 -2.0 -1.0  0.0  1.0  2.0  3.0  4.0  0.0        10180.177
 1.303186606D+02-4.919201960D+01 6.194282930D+00-5.795780180D-02 5.504625810D-04
-2.061041844D-06 2.847398383D-09 0.000000000D+00 5.394886690D+04-2.858552473D+00
    200.000  1000.000 7 -2.0 -1.0  0.0  1.0  2.0  3.0  4.0  0.0        10180.177
-4.703840330D+04 5.955107910D+02-6.666804130D-03 1.620476680D-02-1.627518262D-05
 7.942912160D-09-1.493796005D-12 0.000000000D+00 5.092015770D+04 2.475445798D+01
   1000.000  6000.000 7 -2.0 -1.0  0.0  1.0  2.0  3.0  4.0  0.0        10180.177
-1.136706125D+05-9.057756660D+02 8.126913300D+00-2.278063673D-04 4.570532710D-08
-5.163206090D-12 3.031473359D-16 0.000000000D+00 5.755465440D+04-2.241696262D+01
```

Thermochemical data of NCN with heat of formation at 298K = 457.8 kJ/mol in 7-term-NASA-format:

```
NCN               T 1/12N   2C  1.   0.    0G   200.000  6000.000              1
 5.68743460E+00 1.82663439E-03-7.07551130E-07 1.19517763E-10-7.31862017E-15    2
 5.30454071E+04-6.31950475E+00 2.79807986E+00 1.00008861E-02-9.59242059E-06    3
 4.75565678E-09-1.04348512E-12 5.38574577E+04 8.62129570E+00 5.50603704E+04    4
```

Thermochemical data of NCN with heat of formation at 298K = 457.8 kJ/mol in table format:

T	CP	H-H298	S	-(G-H298)/T	H
K	J/(mol K)	kJ/mol	J/(mol K)	J/(mol K)	kJ/mol
0	-	-10.180			447.620
50	29.110	-8.725	166.624	341.127	449.075
60	29.152	-8.434	171.935	312.499	449.366
70	29.269	-8.142	176.436	292.748	449.658
80	29.498	-7.848	180.358	278.459	449.952
90	29.853	-7.551	183.852	267.756	450.249
100	30.328	-7.251	187.021	259.527	450.549
110	30.902	-6.945	189.937	253.070	450.855
120	31.549	-6.632	192.653	247.923	451.168
130	32.240	-6.313	195.206	243.771	451.487
140	32.952	-5.987	197.621	240.389	451.813
150	33.668	-5.654	199.919	237.615	452.146
160	34.374	-5.314	202.114	235.328	452.486
170	35.062	-4.967	204.219	233.436	452.833
180	35.726	-4.613	206.242	231.870	453.187
190	36.365	-4.253	208.191	230.573	453.547
200	36.977	-3.886	210.072	229.501	453.914
210	37.565	-3.513	211.890	228.619	454.287
220	38.129	-3.135	213.651	227.899	454.665
230	38.671	-2.751	215.358	227.317	455.049
240	39.194	-2.361	217.015	226.853	455.439
250	39.700	-1.967	218.625	226.492	455.833

The original publication is available at http://dx.doi.org/10.1016/j.proci.2012.06.128

T	CP	H-H298	S	-(G-H298)/T	H
K	J/(mol K)	kJ/mol	J/(mol K)	J/(mol K)	kJ/mol
260	40.190	-1.567	220.192	226.220	456.233
270	40.666	-1.163	221.718	226.025	456.637
280	41.131	-0.754	223.205	225.898	457.046
290	41.584	-0.340	224.656	225.830	457.460
298.15	41.946	0.000	225.814	225.814	457.800
300	42.028	0.078	226.073	225.815	457.878
320	42.888	0.927	228.813	225.917	458.727
340	43.715	1.793	231.438	226.165	459.593
360	44.514	2.675	233.960	226.529	460.475
380	45.283	3.573	236.387	226.984	461.373
400	46.024	4.486	238.729	227.513	462.286
420	46.737	5.414	240.992	228.101	463.214
440	47.421	6.356	243.182	228.737	464.156
460	48.077	7.311	245.305	229.412	465.111
480	48.705	8.279	247.364	230.117	466.079
500	49.304	9.259	249.365	230.847	467.059
520	49.875	10.251	251.310	231.597	468.051
540	50.419	11.254	253.202	232.362	469.054
560	50.936	12.267	255.045	233.140	470.067
580	51.428	13.291	256.841	233.926	471.091
600	51.895	14.324	258.593	234.719	472.124
620	52.338	15.366	260.302	235.517	473.166
640	52.759	16.417	261.970	236.318	474.217
660	53.158	17.477	263.600	237.120	475.277
680	53.536	18.544	265.192	237.922	476.344
700	53.895	19.618	266.749	238.724	477.418
720	54.235	20.699	268.272	239.523	478.499
740	54.558	21.787	269.763	240.320	479.587
760	54.864	22.882	271.222	241.115	480.682
780	55.154	23.982	272.651	241.905	481.782
800	55.430	25.088	274.051	242.691	482.888
820	55.691	26.199	275.423	243.473	483.999
840	55.940	27.315	276.768	244.250	485.115
860	56.176	28.436	278.087	245.021	486.236
880	56.400	29.562	279.381	245.787	487.362
900	56.614	30.692	280.651	246.548	488.492
920	56.817	31.827	281.897	247.303	489.627
940	57.010	32.965	283.121	248.052	490.765
960	57.194	34.107	284.323	248.795	491.907
980	57.369	35.253	285.504	249.532	493.053
1000	57.536	36.402	286.665	250.264	494.202
1020	57.695	37.554	287.806	250.988	495.354
1040	57.847	38.709	288.928	251.707	496.509
1060	57.993	39.868	290.031	252.420	497.668
1080	58.131	41.029	291.117	253.127	498.829
1100	58.264	42.193	292.184	253.827	499.993
1120	58.390	43.360	293.235	254.521	501.160
1140	58.511	44.529	294.270	255.210	502.329
1160	58.627	45.700	295.289	255.892	503.500
1180	58.738	46.874	296.292	256.568	504.674
1200	58.845	48.049	297.280	257.239	505.849
1250	59.092	50.998	299.687	258.889	508.798
1300	59.314	53.958	302.009	260.503	511.758
1350	59.516	56.929	304.251	262.082	514.729
1400	59.698	59.910	306.419	263.627	517.710
1450	59.865	62.899	308.517	265.139	520.699
1500	60.016	65.896	310.549	266.619	523.696

T	CP	H-H298	S	-(G-H298)/T	H
K	J/(mol K)	kJ/mol	J/(mol K)	J/(mol K)	kJ/mol
1550	60.154	68.900	312.519	268.068	526.700
1600	60.281	71.911	314.431	269.487	529.711
1650	60.398	74.928	316.288	270.877	532.728
1700	60.505	77.951	318.093	272.239	535.751
1750	60.603	80.978	319.848	273.575	538.778
1800	60.694	84.011	321.557	274.884	541.811
1850	60.779	87.048	323.221	276.168	544.848
1900	60.857	90.089	324.843	277.428	547.889
1950	60.930	93.133	326.424	278.664	550.933
2000	60.997	96.181	327.968	279.877	553.981
2050	61.060	99.233	329.475	281.068	557.033
2100	61.119	102.287	330.947	282.239	560.087
2150	61.174	105.345	332.386	283.388	563.145
2200	61.225	108.405	333.793	284.518	566.205
2250	61.273	111.467	335.169	285.628	569.267
2300	61.318	114.532	336.516	286.720	572.332
2350	61.361	117.599	337.835	287.793	575.399
2400	61.401	120.668	339.128	288.849	578.468
2450	61.438	123.739	340.394	289.888	581.539
2500	61.474	126.812	341.636	290.911	584.612
2550	61.507	129.886	342.853	291.918	587.686
2600	61.539	132.963	344.048	292.909	590.763
2650	61.569	136.040	345.221	293.885	593.840
2700	61.597	139.119	346.372	294.846	596.919
2750	61.624	142.200	347.502	295.793	600.000
2800	61.650	145.282	348.613	296.727	603.082
2850	61.674	148.365	349.704	297.646	606.165
2900	61.697	151.449	350.777	298.553	609.249
2950	61.719	154.535	351.832	299.447	612.335
3000	61.740	157.621	352.869	300.329	615.421
3050	61.760	160.709	353.890	301.199	618.509
3100	61.779	163.797	354.895	302.057	621.597
3150	61.798	166.887	355.883	302.903	624.687
3200	61.815	169.977	356.857	303.739	627.777
3250	61.832	173.068	357.815	304.563	630.868
3300	61.848	176.160	358.759	305.377	633.960
3350	61.864	179.253	359.689	306.181	637.053
3400	61.879	182.346	360.606	306.975	640.146
3450	61.894	185.441	361.509	307.759	643.241
3500	61.908	188.536	362.400	308.533	646.336
3550	61.921	191.632	363.278	309.298	649.432
3600	61.935	194.728	364.145	310.053	652.528
3650	61.947	197.825	364.999	310.800	655.625
3700	61.960	200.923	365.842	311.538	658.723
3750	61.972	204.021	366.674	312.268	661.821
3800	61.984	207.120	367.495	312.989	664.920
3850	61.996	210.219	368.305	313.702	668.019
3900	62.008	213.320	369.105	314.408	671.120
3950	62.019	216.420	369.895	315.105	674.220

T	CP	H-H298	S	-(G-H298)/T	H
K	J/(mol K)	kJ/mol	J/(mol K)	J/(mol K)	kJ/mol
4000	62.031	219.521	370.675	315.795	677.321
4050	62.042	222.623	371.446	316.477	680.423
4100	62.053	225.726	372.207	317.152	683.526
4150	62.064	228.829	372.959	317.820	686.629
4200	62.076	231.932	373.703	318.481	689.732
4250	62.087	235.036	374.437	319.135	692.836
4300	62.098	238.141	375.164	319.782	695.941
4350	62.109	241.246	375.882	320.423	699.046
4400	62.120	244.352	376.591	321.057	702.152
4450	62.131	247.458	377.293	321.685	705.258
4500	62.143	250.565	377.988	322.307	708.365
4550	62.154	253.672	378.674	322.922	711.472
4600	62.166	256.780	379.354	323.532	714.580
4650	62.178	259.889	380.026	324.136	717.689
4700	62.190	262.998	380.691	324.734	720.798
4750	62.202	266.108	381.349	325.326	723.908
4800	62.214	269.218	382.001	325.913	727.018
4850	62.227	272.329	382.645	326.495	730.129
4900	62.240	275.441	383.284	327.071	733.241
4950	62.253	278.553	383.916	327.642	736.353
5000	62.266	281.666	384.541	328.208	739.466
5050	62.280	284.780	385.161	328.769	742.580
5100	62.293	287.894	385.775	329.325	745.694
5150	62.308	291.009	386.382	329.876	748.809
5200	62.322	294.125	386.985	330.422	751.925
5250	62.337	297.241	387.581	330.964	755.041
5300	62.352	300.359	388.172	331.500	758.159
5350	62.367	303.477	388.757	332.033	761.277
5400	62.383	306.595	389.338	332.561	764.395
5450	62.398	309.715	389.913	333.084	767.515
5500	62.415	312.835	390.483	333.604	770.635
5550	62.431	315.956	391.048	334.119	773.756
5600	62.448	319.078	391.608	334.629	776.878
5650	62.466	322.201	392.163	335.136	780.001
5700	62.483	325.325	392.713	335.639	783.125
5750	62.501	328.450	393.259	336.137	786.250
5800	62.519	331.575	393.800	336.632	789.375
5850	62.538	334.701	394.337	337.123	792.501
5900	62.557	337.829	394.869	337.610	795.629
5950	62.576	340.957	395.397	338.094	798.757
6000	62.596	344.086	395.921	338.573	801.886

References

[1] C. P. Fenimore, Proc. Combust. Inst., 13 (1971) 373-380.

[2] J. A. Miller, C. T. Bowman, Prog. Energy Combust. Sci. 15 (1989) 287-338.

[3] L. Cui, K. Morokuma, J. M. Bowman, S. J. Klippenstein, J. Chem. Phys. 110 (1999) 9469-9482.

[4] L.V. Moskaleva, M.C. Lin, Proc. Combust. Inst. 28 (2000) 2393-2401.

[5] L. B. Harding, S. J. Klippenstein, J. A. Miller, J. Phys. Chem. A, 112 (2008) 522-532.

[6] V. Vasudevan, R. K. Hanson, C. T. Bowman, D. M. Golden, and D. F. Davidson J. Phys. Chem. A, 111 (2007) 11818-11830.

[7] A. El Bakali, L. Pillier, P. Desgroux, B. Lefort , L. Gasnot , J.F. Pauwels, I. da Costa, Fuel 85 (2006) 896–909.

[8] J. A. Sutton, B. A. Williams, J. W. Fleming, Combustion and Flame 153 (2008) 465–478.

[9] A. A. Konnov, Combustion and Flame 156 (2009) 2093–2105.

[10] E. P. Clifford, P. G. Wenthold, W. C. Lineberger, G. A. Petersson, and G. B. Ellison., J. Phys. Chem. A, 101 (1997) 4338-4345.
E. P. Clifford, P. G. Wenthold, W. C. Lineberger, G. A. Petersson, K. M. Broadus, S. R. Kass, S. Kato, C. H. DePuy, V. M. Bierbaum, and G. B. Ellison, J. Phys. Chem. A, 102 (1998) 7100-7112

[11] R. T. Bise, H. Choi, and D. M. Neumark, J. Chem. Phys. 111 (1999) 4923-4932.

[12] S. Canneaux, A. Wallet, M. Ribaucour, and F. Louis, Comput. Theor. Chem. 967 (2011) 67-74.

[13] N. Lamoureux, P. Desgroux, A. El Bakali, J. F. Pauwels, Combustion and Flame 157 (2010) 1929–1941.

[14] B. Ruscic, R. E. Pinzon, M. L. Morton, G. von Laszewski, S. Bittner, S. G. Nijsure, K. A. Amin, M. Minkoff, and A. F. Wagner, J. Phys. Chem. A 108 (2004) 9979-9997

[15] B. Ruscic, R. E. Pinzon, G. von Laszewski, D. Kodeboyina, A. Burcat, D. Leahy, D. Montoya, and A. F. Wagner, J. Phys.: Conf. Ser. 16 (2005) 561-570.

[16] E. Goos, A. Burcat and B. Ruscic, "Extended Third Millennium Ideal Gas and Condensed Phase Thermochemical Database for Combustion with updates from Active Thermochemical Tables"; available at ftp://ftp.technion.ac.il/pub/supported/aetdd/thermodynamics/
(mirrored at http://garfield.chem.elte.hu/Burcat/burcat.html), and also available from DLR webpage http://www.dlr.de/vt/en/;
last printed version: A. Burcat and B. Ruscic, "Third Millennium Ideal Gas and Condensed Phase Thermochemical Database for Combustion with updates from Active Thermochemical Tables", ANL Report 05/20 and TAE Report 960 (2005).

[17] B. Ruscic, results obtained from Active Thermochemical Tables using the Core Thermochemical Network version 1.112, see [16].

[18] W. R. Stevens, B. Ruscic, and T. Baer, J. Phys. Chem. A 114 (2010) 13134-13145.

[19] G. Dixon-Lewis, P. Marshall, B. Ruscic, A. Burcat, E. Goos, A. Cuoci, A. Frassoldati, T. Faravelli, and P. Glarborg, Combust. Flame 159 (2012) 528-540.

[20] R. Sivaramakrishnan, J. V. Michael, and B. Ruscic, Int. J. Chem. Kin. 44, (2012) 194–205.

[21] E. Goos, A. Burcat, *Thermochemistry*, in *Handbook of Combustion* Vol. 1, p. 135-152; M. Lackner, F.

Winter, A. K. Agarwal (Eds.) 2010, Wiley and Sons, VCH.

[22] E. Goos, A. Burcat, *Overview of Thermochemistry and its Application to Reaction Kinetics*, in "*Rate Constant Calculation for Thermal Reactions: Methods and Applications*", p. 3-32, H. DaCosta, M. Fan (Eds.), 2012, John Wiley & Sons. (http://media.wiley.com/product_data/excerpt/08/04705823/0470582308-186.pdf)

[23] B. J. McBride and S. Gordon, Computer Program for Calculating and Fitting Thermodynamic Functions, NASA Report 1271 (1992).

[24] M. E. Jacox, Vibrational and Electronic Energy Levels of Polyatomic Transient Molecules, Supplement A, J. Phys. Chem. Ref. Data, **27** (1998) 115-393.

[25] K. Hoyermann, F. Mauß, T. Zeuch, Phys. Chem. Chem. Phys. 6 (2004) 3824-3835.

[26] S. S. Ahmed, F. Mauss, G. Moréac, T. Zeuch, Phys. Chem. Chem. Phys. 9 (2007) 1107-1126.

[27] J. Li, Z. Zhao, A. Kazakov, M. Chaos, F. L. Dryer, J. J. Scire Jr., Int. J. Chem. Kinet. 39 (2007) 109-136.

[28] S. S. Ahmed, F. Mauss, T. Zeuch, Z. Phys. Chem. 223 (2009) 551-563.

[29] P. Oßwald, K. Kohse-Höinghaus, U. Struckmeier, T. Zeuch, L. Seidel, L. Leon, F. Mauss, Z. Phys. Chem. 225 (2011) 1029-1054.

[30] I. G. Zsély, J. Zádor, T. Turányi, Int. J. Chem. Kinet. 40 (2008) 754–768.

[31] http://www.loge.se/Products/DARS-Basic.html.

[32] L. V. Gurvich, I. V. Veyts, and C. B. Alcock, "Thermodynamic Properties of Individual Substances", Vol. 1, Parts 1 and 2, Hemisphere, New York, 1989; id., Vol. 2, Parts 1 and 2, Hemisphere, New York, 1991.

[33] M. W. Chase Jr., Ed. "NIST-JANAF Thermochemical Tables", 4th ed., J. Phys. Chem. Ref. Data, Monograph 9 (1998).

[34] H. Okabe and A. Mele, J. Chem. Phys. 51 (1969) 2100-2106.

[35] NIST Chemistry WebBook, NIST Standard Reference Database Number 69, Eds. P.J. Linstrom and W.G. Mallard, National Institute of Standards and Technology, Gaithersburg MD, 20899, http://webbook.nist.gov, (retrieved December 2011).

[36] J. M. L. Martin, P. R. Taylor, J. P. Francois, and R. Gijbels, Chem. Phys. Lett. 226 (1994) 475-483.

37 T. R. Taylor, R. T. Bise, K. R. Asmis, and D. M. Neumark, Chem. Phys. Lett. 301 (1999) 413-416.

[38] B. Ruscic, J. V. Michael, P. C. Redfern, L. A. Curtiss, and K. Raghavachari, J. Phys. Chem. A 102 (1998) 10889-10899.

[39] B. Ruscic, M. Litorja, and R. L. Asher, J. Phys. Chem. A 103 (1999) 8625-8633.

[40] B. Ruscic, J. E. Boggs, A. Burcat, A. G. Csaszar, J. Demaison, R. Janoschek, J. M. L. Martin, M. L. Morton, M. J. Rossi, J. F. Stanton, P. G. Szalay, P. R. Westmoreland, F. Zabel, and T. Berces, J. Phys. Chem. Ref. Data 34 (2005) 573-588.

[41] T. Zeuch, G. Moréac, S. S. Ahmed, F. Mauss, Combustion and Flame, 155 (2008) 651-674.

[42] W. Hack, M. Hold, K. Hoyermann, J. Wehmeyer, T. Zeuch, Phys. Chem. Chem. Phys. **7** (2005) 1977-1984.

[43] R.P. Lindstedt, G. Skevis, Combust. Sci. Technol. 125 (1–6) (1997) 73–137.

[44] a.) http://www.grc.nasa.gov/WWW/CEAWeb/ceaHome.htm, accessed 30. July 2012.
b.) B. J. McBride, M. J. Zehe, S. Gordon, NASA Glenn coefficients for Calculating Thermodynamic

Properties of Individual Species (2002) Glenn Research Center, Cleveland, Ohio, NASA TP – 2002-211556.

[45] V. M. Zamansky and V. V. Lissianski, Minimization of carbon loss in coal reburning, Semiannual Report No. 2 for Period February 11 - August 10, 2001, September 7, 2001, DOE Contract No. DE-FC26-00NT40912, General Electric Energy and Environmental Research Corporation (GE EER).

[46] S. Garner, T. Dubois, C. Togbé, N. Chaumeix, P. Dagaut, K. Brezinsky, Combustion and Flame, 158 (2011) 2302-2313.

[47] a.) R.S. Zhu, M.C. Lin, Int. J. Chem. Kinet. 37 (2005) 593-598.
b.) R.S. Zhu, M.C. Lin, J. Phys. Chem. A 111 (2007) 6766-6771.
c.) R.S. Zhu, H.M.T. Nguyen, M.C. Lin, J. Phys. Chem. A 113 (2008) 298-304.

[48] A. M. Mebel, K. Morokuma, M.C. Lin, J. Chem. Phys. 103 (1995) 7414–7421.

[49] S. Gersen, A.V. Mokhov, H.B. Levinsky, Combustion and Flame 155 (2008) 267–276.

[50] a.) A. V. Sepman, A. V. Mokhov and H. B. Levinsky, Int. J. Hydrogen Energy **36**, (2011) 4474–4481.
b.) A.V. Sepman, A.V. Mokhov and H.B. Levinsky, Int. J. Hydrogen Energy, 36 (2011) 13831-13837.

[51] D.J. Benard, C. Linnen, A. Harker, H.H. Michels, J.B. Addison, R. Ondercin, J. Phys. Chem. B 102 (1998) 6010-6019.

[52] a.) S. Xu, M.C. Lin, J. Phys. Chem. A 111 (2007) 6730-6740.
b.) S. Xu, M.C. Lin, Proc. Combust. Inst. 32 (2009) 99-106.

[53] R.S. Zhu, S.C. Xu, M.C. Lin, Chem. Phys. Lett. 488 (2010) 121-125.

[54] C.F. Melius, Thermochemistry and Reaction Mechanisms of Nitromethane Ignition, Journal de Physique IV – Proceedings 05 (C4) C4-535 (1995), DOI : 10.1051/jp4:1995443.

[55] a.) P. Dagaut P. Glarborg, M. U. Alzueta, The oxidation of hydrogen cyanide and related chemistry, Progress in Energy and Combustion Science 34 (2008) 1–46.
b.) NCN thermodynamical data of [55a] provided in NASA format, but not used, e.g. in S. M. Sarathy, M. J. Thomson, C. Togbé, P. Dagaut, F. Halter, C. Mounaim-Rousselle, An experimental and kinetic modeling study of n-butanol combustion, Combustion and Flame 156 (2009) 852–864.

[56] M. Hori, and N. Matsunaga, N. Marinov, W. Pitz, C. Westbrook, Proceedings of the Combustion Institute, Volume 27 (1998) 389-396.

[57] J. Dammeier and G. Friedrichs, J. Phys. Chem. A 114 (2010) 12963–12971.